SIMULATION OF SEMICONDUCTOR DEVICES AND PROCESSES Vol. 4
Edited by W. Fichtner, D. Aemmer - Zurich (Switzerland) September 12-14, 1991 - Hartung-Gorre

A Self-Consistent Discretization Scheme for Current and Energy Transport Equations

Datong Chen[1], Edwin C. Kan, Umberto Ravaioli,
Beckman Institute, Univ. of Illinois at Urbana-Champaign,
405 North Mathews Ave., Urbana, IL 61801, USA

Zhiping Yu and Robert W. Dutton
Integrated Circuits Laboratory, Stanford University,
231 AEL Building, Stanford, CA 94305, USA

Abstract

We propose a discretization scheme which implements the box integration / Scharfetter-Gummel method for a new Energy Transport model. The discretization treats consistently the current and energy flux and avoids typical problems encountered in many hydrodynamic formulations. Simulation results are satisfactory from both the numerical and physical points of view.

1 Introduction

In recent years, much effort [1]-[5] has focused on extending the Scharfetter-Gummel (S-G) scheme [6], which results in excellent numerical stability and retains reasonable accuracy in Drift-Diffusion simulation, to the case including the energy transport equation (e.g. hydrodynamic (HD) models). However, these discretization methods are not truly self-consistent in terms of current and energy flux, since the assumptions used in discretizing the local energy transport equations, are different from those in the local current equations. In addition, the resulting formulations of the energy balance equation pose considerable difficulties in the numerical implementation.

We discuss here the discretization of a novel Energy Transport (ET) model [7] briefly described in Sec. II, which avoids the direct use of the phenomenological Wiedmann-Franz law in conventional HD models and employs an elegant parallel between the expressions for the current and the energy flux. The self-consistent discretization scheme based on the ET model is a natural extension of the S-G scheme and has been implemented in a 2-D simulator. To demonstrate the features of this model, we compare our numerical results with HD simulations, for the well known case of Si n^+-n-n^+ test structures.

2 Physical Model

The 0th and 2nd order moments of the BTE give the carrier continuity and energy balance equations:

$$\nabla \cdot \mathbf{J} = G - R\,; \tag{1}$$

[1]Current address: Integrated Circuits Labs, Stanford University, 231 AEL, Stanford, CA 94305

$$\nabla \cdot \mathbf{S} = \mathbf{F} \cdot \mathbf{J} - n < \left.\frac{\partial E}{\partial t}\right|_{coll} > \tag{2}$$

where $\mathbf{F}$ is the electric field, $\mathbf{J} = -qn < \mathbf{v} >= -q \int d^3k\mathbf{v}f$ and $\mathbf{S} = n < E\mathbf{v} >= \int d^3k\, E\mathbf{v}f$. Here, q is the elementary charge, n is the carrier concentration, $\mathbf{v}$ is the carrier velocity, $\mathbf{k}$ is the crystal momentum, f is the distribution function and E is the carrier energy. To derive $\mathbf{J}$ and $\mathbf{S}$ from the BTE as functionals of n and $< E >$, the distribution function f is decomposed as $f = f_0 + f_1$ with f_0 and f_1 as even and odd functions, respectively. We further use the microscopic relaxation time approximation for the collision term, $(\partial f/\partial t)_{coll} = -f_1/\tau$, assuming $f_1 \ll f_0$ (as given for instance by Stratton [8]) and then obtain

$$f_1 = \frac{q\tau\mathbf{F}}{\hbar}\nabla_{\mathbf{k}} f_0 - \tau\mathbf{v}\nabla_{\mathbf{r}} f_0 \,. \tag{3}$$

Substitution of (3) into the expressions for $\mathbf{J}$ and $\mathbf{S}$ will yield

$$\mathbf{J} = -q\int d^3k\mathbf{v}f_1 = q(n\hat{\mu}\mathbf{F} + \nabla \cdot (n\hat{D}))\,; \tag{4}$$

$$\mathbf{S} = \int d^3k\, E\mathbf{v}f_1 = -n\hat{\mu}^E\mathbf{F} - \nabla \cdot (n\hat{D}^E)\,, \tag{5}$$

which resemble the perturbed BTE solution approach in [9]. The transport coefficients $\hat{\mu}$, $\hat{D}$, $\hat{\mu}^E$, and $\hat{D}^E$, all of which we can model as functions of $< E >$, are tensors and can be determined from the knowledge of f_0. The divergence of tensor in (4) and (5) means to take the divergence of each row of the tensor as a vector element. The following approximations for $f_0(\mathbf{k})$ and the energy $E(\mathbf{k})$ are used to obtain a complete set of transport coefficients:

1) nonparabolic bands: $\hbar^2\mathbf{k}^2/2m^* = E(1+\alpha E)$;
2) non-Maxwellian effects: $f_0 = (1+\gamma E/k_BT_e)f_m(E)$, where $f_m(E)$ is the Maxwellian distribution at an elevated temperature T_e and γ is the non-Maxwellian parameter;
3) field-induced anisotropy [10]: $f_0(\mathbf{k}) = \frac{1}{2}[f_m(E(\mathbf{k}+\mathbf{k}_0)) + f_m(E(\mathbf{k}-\mathbf{k}_0))]$.

It is very important to notice that in this approach all of the necessary transport parameters can be determined, for instance, from bulk Monte Carlo simulations and that the Wiedmann-Franz law for heat flow is *never* invoked, as it is necessary in the conventional hydrodynamic method.

3 Discretization Scheme

For Si, the correction from the field-induced anisotropy is generally not important [10]. With assumptions 1) and 2) above, $\hat{\mu}$, $\hat{D}$, $\hat{\mu}^E$, and $\hat{D}^E$ will degenerate to scalar forms and the modified Einstein relations are valid between μ and D and between μ^E and D^E

$$D = \frac{k_BT_m}{q}\mu\,; \tag{6}$$

$$D^E = \frac{k_BT_m}{q}\mu^E \tag{7}$$

where $T_m = (1+\gamma)T_e$ is an approximation for the carrier temperature with the relation to the mean carrier energy as

$$< E > \simeq (1 + \frac{5}{2}\alpha k_BT_m)\frac{3}{2}k_BT_m\,. \tag{8}$$

Furthermore, μ and μ^E are related by

$$\mu^E = (\frac{5}{2} - p)(1 - \frac{\alpha k_B T_m}{2}) k_B T_m \mu = C_e k_B T_m \mu \quad (9)$$

where p depends on the dominant scattering mechanism and is derived from the power law of the microscopic relaxation time, $\tau(\mathbf{k}) \simeq \tau(E) \propto E^{-p}$. The parameter p is constant for a Maxwellian-like distribution and is a slowly varying function of the mean carrier energy for a non-Maxwellian distribution, which ranges from 0.5 to 1.0 according to our bulk Monte Carlo simulations. Substituting (6), (7) and (9) into (4) and (5), we can write the normalized expressions for $\mathbf{J}$ and $\mathbf{S}$ as

$$\tilde{\mathbf{J}} = -N \nabla \psi + \nabla (NT) ; \quad (10)$$

$$\tilde{\mathbf{S}} = -NT \nabla \psi + \nabla (NT^2) \quad (11)$$

where $N = n\mu$, T is the carrier temperature normalized to the lattice temperature T_0, and ψ is the electrical potential. The similarity of the functional expressions in (10) and (11) serves as the basis for our extended Scharfetter-Gummel discretization for both continuity and energy balance equations. In order to perform the standard box integration around each discretization node, we need to know $\tilde{\mathbf{J}}$ and $\tilde{\mathbf{S}}$ along each grid line. On the mesh line connecting the nodes i and j, (10) and (11) can be expressed as:

$$\tilde{J}_l = -N \frac{d\psi}{dl} + \frac{d(NT)}{dl} ; \quad (12)$$

$$\tilde{S}_l = -NT \frac{d\psi}{dl} + \frac{d(NT^2)}{dl} \quad (13)$$

where l is a coordinate defined on the mesh line. By using the following assumptions

1) $\tilde{J}_l$ and $\tilde{S}_l$ are constants
2) $(1/T)(d\psi/dl)$ is a constant

we can solve both (12) and (13), and obtain

$$\tilde{J}_l = \frac{1}{L_{ij}} \frac{u_{ij}}{\sinh(u_{ij})} (e^{-u_{ij}} N_j T_j - e^{u_{ij}} N_i T_i) ; \quad (14)$$

$$\tilde{S}_l = \frac{1}{L_{ij}} \frac{u_{ij}}{\sinh(u_{ij})} (e^{-u_{ij}} N_j T_j^2 - e^{u_{ij}} N_i T_i^2) \quad (15)$$

where L_{ij} is the distance between nodes i and j, and $u_{ij} = (\psi_j - \psi_i)/2 < T >$. T is normally a slowly–varying function of space, therefore the assumption of constant $(1/T)(d\psi/dl)$ is justified. For instance, the approximation $< T > = (T_i + T_j)/2$ can be reasonable in practice. Moreover, the joule heating term in (2), $\mathbf{F} \cdot \mathbf{J}$, can be included in the divergence operator by $\mathbf{F} \cdot \mathbf{J} = -\nabla \cdot (\psi \mathbf{J}) + \psi \nabla \cdot \mathbf{J}$. If we define $\mathbf{H} = \mathbf{S} + \psi \mathbf{J}$ with the energy relaxation time approximation, (2) will become

$$\nabla \cdot \mathbf{H} = \nabla \cdot (\mathbf{S} + \psi \mathbf{J}) = \psi \cdot (G - R) - n \frac{< E > - E_0}{\tau_\epsilon} \quad (16)$$

where $E_0 = 3k_B T_0/2$ and τ_ϵ is the energy relaxation time. The final normalized expression used in the fluxes through the sides of the finite boxes for the energy balance equation can be written as

$$\begin{aligned} \tilde{H}_l &= -C_e \tilde{S}_l + \psi \tilde{J}_l \\ &= \frac{1}{L_{ij}} \frac{u_{ij}}{\sinh(u_{ij})} \left(e^{-u_{ij}} N_j T_j (\frac{\psi_i + \psi_j}{2} - C_e T_j) - e^{u_{ij}} N_i T_i (\frac{\psi_i + \psi_j}{2} - C_e T_i) \right) . \end{aligned} \quad (17)$$

4 Simulation Results

The new discretization method has been implemented in a 2-D device simulator based on the improved ET model using the full Newton method. Numerical tests have been carried out for a Si $n^+ - n - n^+$ structure with a 0.4 μm n region (see Fig. 1 and 2). Here the mobility model is chosen as $\mu(T_m) = \mu_0 T_0 / T_m$, where μ_0 is the low-field mobility. The energy relaxation time τ_ϵ is presently chosen as a constant. In both figures we vary p for illustration of the typical spurious velocity overshoot problem in the conventional HD models [11, 12]. In our formulation, the spurious peak is not only much reduced but also rather insensitive to the selection of p in contrary to the usual HD models. However, the accurate estimation of the velocity in the n region greatly depends on p. This indicates that p should not be chosen randomly to eliminate the spurious peak as in many HD models. We can alternatively use $p(T_m)$, extracted from the bulk MC results, in a more sophisticated model. The improved ET model appears very stable numerically. Quadratic convergence of the full Newton Scheme has been observed for every case with a good initial guess. We would like to point out again that non-parabolicity effects are already included in the formulation of the ET model. For GaAs device modeling, the field-induced anisotropy effect can also be included with little modification.

5 Acknowledgements

This work is supported by the Joint Services Electronics Program(JSEP) under the contract no. N0001490-J-1270, and by the National Science Foundation(NSF) through the National Center for Computational Electronics(NCCE) grant no. NSFEET8719100, and by the Semiconductor Research Corporation(SRC) under the contract no. 90-DJ116. The authors would like to thank Prof. Thomas Kerkhoven of University of Illinois, Prof. Joseph W. Jerome of Northwestern University and Prof. Chi-Wang Shu of Brown University for fruitful discussions.

References

[1] T. W. Tang, 'Extension of the Scharfetter-Gummel Algorithm to the Energy Balance Equation, ' *IEEE Trans. on Electron Devices*, vol. ED-31, no. 12, pp. 1912–1914, 1984.

[2] C. C. McAndrew, K. Singhal and E. L. Heasell, 'A Consistent Nonisothermal Extension of the Scharfetter-Gummel Stable Difference Approximation, ' *IEEE Electron Device Lett.*, vol. EDL-6, no. 9, pp. 446-447, 1985.

[3] M. Rudan and F. Odeh, 'Multi-dimensional Discretization Scheme for the Hydrodynamic Model of Semiconductor Devices, ' *COMPEL*, vol. 5, no. 3, pp. 149-183, 1986.

[4] S. Szeto and R. Reif, 'Asymptotic Electron Energy Flux Equations for Hot-Carrier Transport Simulation, ' *IEEE Electron Device Lett.*, vol. EDL-8, no. 8, pp. 336-337, 1987.

[5] A. Forghieri, R. Guerrieri, Paolo Ciampolini, A. Gnudi, M. Rudan and G. Baccarani, 'A New Discretization Strategy of the Semiconductor Equations Comprising Momentum and Energy Balance, ' *IEEE Trans. on CAD*, vol. 7, no. 2, pp. 231-242, 1988.

[6] D. L. Scharfetter and H. K. Gummel, 'Large-Signal Analysis of a Silicon Read Diode Oscillator, ' *IEEE Trans. on Electron Devices*, vol. ED-16, no. 1, pp. 64-77, 1969.

[7] D. Chen, E. C. Kan and U. Ravaioli, 'An Improved Energy Balance Model for Hot-Electron Device Simulation, ' submitted for publication.

[8] R. Stratton, 'Diffusion of Hot and Cold Electrons in Semiconductor Barriers, ' *Physical Review,* vol. 126, no. 6, pp. 2002-2014, Jun. 1962.

[9] C. C. McAndrew, E. L. Heasell and K. Singhal, 'A Comprehensive Transport Model for Semiconductor Device Simulation, ' *Semicond. Sci. and Tech.*, vol. 2, pp. 643-648, 1987.

[10] D. Chen, E. C. Kan and K. Hess, 'Field-Induced Anisotropic Distribution Functions and Semiconductor Transport Equations with Tensor-form Coefficients, ' *J. Appl. Phys.*, vol. 68(10), pp. 5360-5362, Nov. 1990.

[11] A. Gnudi, F. Odeh and M. Rudan, 'Investigation of Non-local Transport Phenomena in Small Semiconductor Devices, ' to be published.

[12] E. Fatemi and J. Jerome, 'Solution of the Hydrodynamic Device Model Using High-Order Nonoscillatory Shock Capturing Algorithms, ' *IEEE Trans. on CAD*, vol. 10, no. 2, 1991.

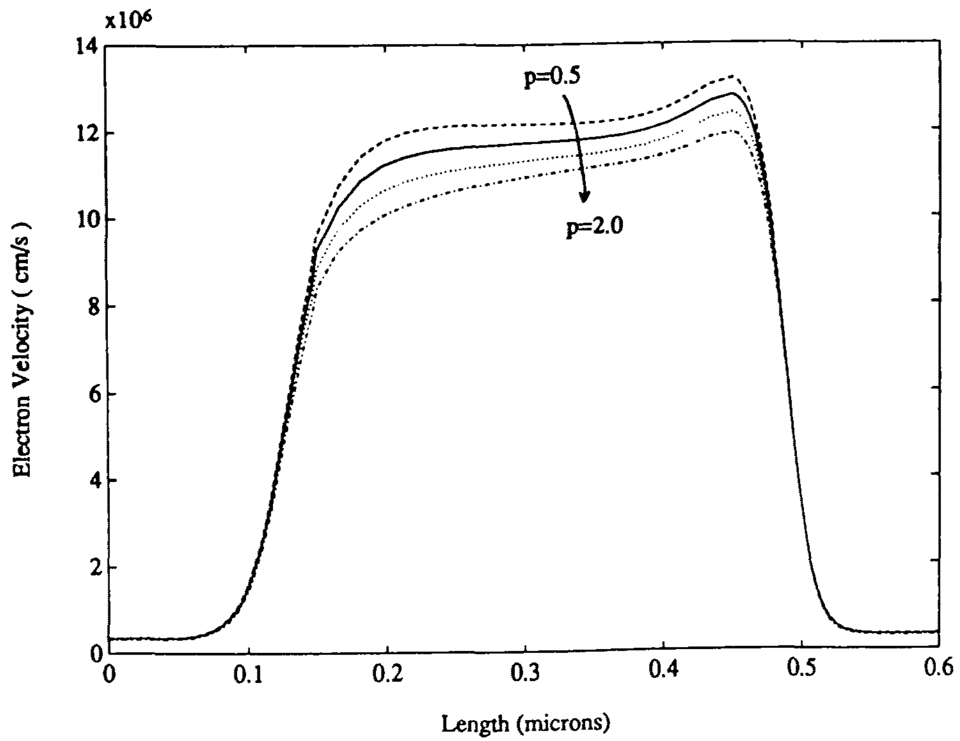

Figure 1: Profiles of electron velocity in a Si $n^+ - n - n^+$ structure with a 0.4 μm n region and doping levels $n^+ = 5\text{x}10^{17} cm^{-3}$, $n = 2\text{x}10^{15} cm^{-3}$, with $p = 0.5, 1.0, 1.5$ and 2.0.

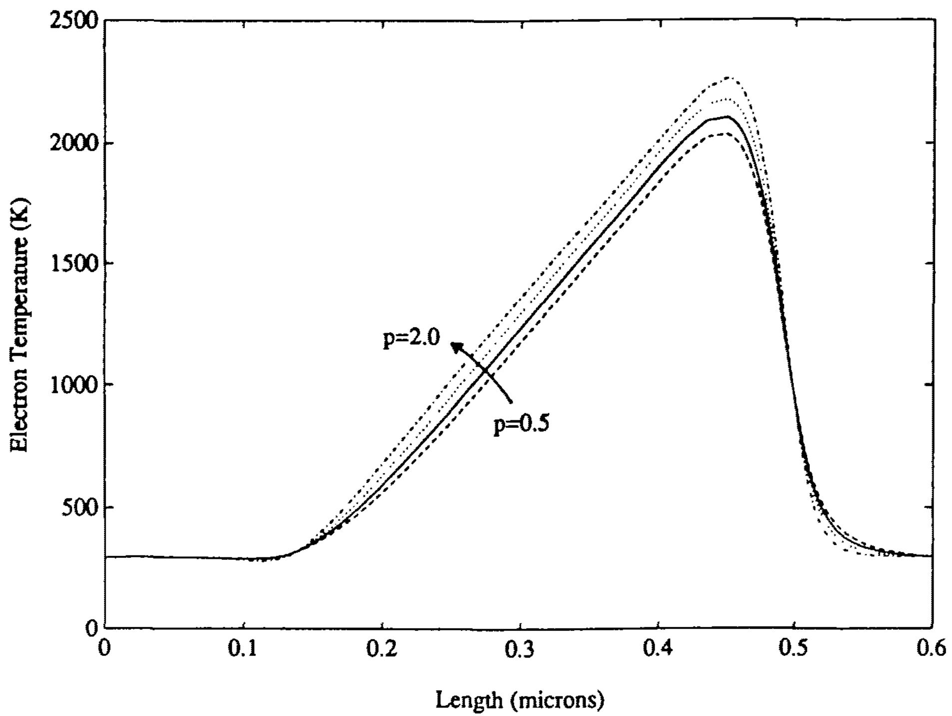

Figure 2: Distribution of the electron temperature for the structure in Fig. 1.